Particle Accelerators, 1994, Vol. 45, pp. 95–110
Reprints available directly from the publisher
Photocopying permitted by license only

A NEW METHOD FOR CALCULATION OF LOW-FREQUENCY COUPLING IMPEDANCE

S.S.KURENNOY and G.V. STUPAKOV

Superconducting Super Collider Laboratory, Dallas, Texas 75237, USA*

(Received 25 June 1993; in final form 2 March 1994)

In high-energy proton accelerators and storage rings the bunch length is typically at least a few times larger than the radius of the vacuum chamber. For example, the Superconducting Super Collider (SSC) will have an rms bunch length above 6cm and a beam-pipe radius below 2cm. The main concern for beam stability in such a machine is the low-frequency impedance, i.e., the coupling impedance at frequencies well below the cut-off frequency of the vacuum chamber. A new analytical approach is developed for calculation of the low-frequency impedance of axisymmetric structures that allows quick and reliable estimates of contributions to the impedance from various chamber discontinuities. Simple formulae for the longitudinal impedance of some typical discontinuities are obtained.

KEY WORDS: Collective effects, electromagnetic field calculations, impedances

1 INTRODUCTION

The low-frequency impedance of axisymmetric structures has been studied by different approaches. In Reference 1 a matching method was applied to study the case of a beam pipe with a cylindrical cavity, and a formula for the inductance of a small pillbox was derived. The numerical solution of the Maxwell equations in time-domain with the TBCI code[2] allows one to obtain the wake potential of a bunch in such structures. The dependence of the inductance of small pillboxes and irises on their geometrical parameters was derived from fitting numerical results obtained by means of TBCI in Reference 3. In a similar way, formulae for the inductance of triangular-shaped insertions were obtained in Reference 4 using the semianalytical integral-equation approach. While practically important, these results do not represent a regular method for obtaining impedances of different structures. This paper aims to fill this apparent gap and to develop a theory that allows effective derivation of the low-frequency impedance for small discontinuities on the beam pipe.

We will consider axisymmetric structures that consist of an infinitely long, perfectly conducting smooth pipe that has a localized discontinuity (e.g., a pillbox or an iris) on it. The frequency under consideration is much below the cut-off frequency of the pipe,

* Operated by the Universities Research Association, Inc., for the U.S. Department of Energy under Contract No.DE-AC35-89ER40486.

$\omega \ll c/b$. In this limit, we show that the calculation of low-frequency impedance is reduced to solution of two quasistatic problems — electrostatic and magnetostatic ones. Assuming additionally that dimensions of the discontinuity (its width g and height h) are much smaller than the pipe radius b, we are able to use conformal mapping for solution of the electrostatic problem and to derive simple formulae for the impedance of several shapes of discontinuities. Comparison with numerical calculations using TBCI shows very good accuracy of our theory in the range of its validity.

2 THE PRINCIPLES BEHIND THE METHOD

To evaluate the coupling impedance, we have to calculate the fields induced in the vacuum chamber by a given current perturbation. Let the current harmonic

$$\vec{I}(z,t) = I_0 \vec{e}_z \exp(ikz - i\omega t) , \tag{1}$$

where $k = \omega/c$, propagate along the chamber axis. If one finds the scattered-field harmonic $E_z = E(r,z)$ (hereafter we omit the time factor $\exp(-i\omega t)$), then the longitudinal impedance is given by (see, for example, reviews in Reference 5)

$$Z(\omega) = -\frac{\mathcal{E}}{I_0} = -\frac{1}{I_0}\int_{-\infty}^{\infty} dz E(r,z)\exp(-ikz) , \tag{2}$$

where $\mathcal{E}$ is the Fourier harmonic of the induced voltage. For axisymmetric structures the monopole longitudinal impedance does not depend on the transverse displacement of the integration path, i.e., the integral in the RHS is independent of r. Since the current wavelength is large compared to the discontinuity size (low frequencies), the beam fields near the pill-box vary slowly and can be treated as almost static ones.

One can easily find the magnetic contribution to $\mathcal{E}$. For cavities, shown in Figures 1(a) and 1(b), the beam azimuthal magnetic field $B_\varphi(r) = \mu_0 I_0/(2\pi r)$ fills the volume of the cavity, therefore, the presence of the pillbox produces an additional magnetic flux

$$\Phi = \iint_S B_\varphi(r) dS , \tag{3}$$

where the integration goes over the cross section S of the enlargement. Using the smallness of the dimensions of the cavity, we can simply put $\Phi \simeq B_\varphi(b)S$. From Faraday's law we can easily find the contribution of the solenoidal electric field, produced by oscillations of this flux with time, to the induced voltage (electromotive force) as

$$\mathcal{E}_{(m)} = i\omega\Phi . \tag{4}$$

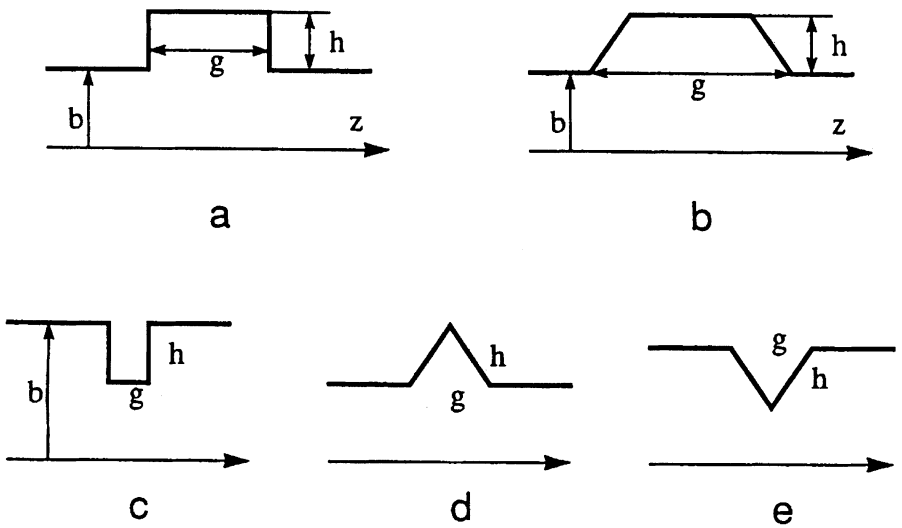

FIGURE 1: Discontinuities of the vacuum chamber.

From the physical point of view the additional magnetic flux due to the enlargement can be treated as if produced by a toroidal solenoid, having the cross section of the cavity, and attached to the smooth pipe. This solenoid is characterized by a dipole magnetic moment $M = 2\pi b\Phi/\mu_0$. The magnetic moment is uniformly distributed along the circumference of the solenoid and has only an azimuthal component. Let us introduce the magnetic moment per unit length, $m = M/(2\pi b)$, and magnetic polarizability of the discontinuity α_m per unit length of circumference as $m = \alpha_m H_\varphi(b)$. Then $\alpha_m = \Phi/(\mu_0 H_\varphi(b))$, and in the case of a small pillbox, $\alpha_m = S$. Respectively, the magnetic contribution to the impedance takes the form

$$Z_{(m)}(\omega) = -\frac{\mathcal{E}_{(m)}}{I_0} = -i\omega\frac{Z_0\alpha_m}{2\pi bc}\,, \tag{5}$$

where μ_0 is replaced by Z_0/c, $Z_0 = 120\pi\ \Omega$. Substituting $\alpha_m = S$ we get the well-known inductive impedance of a small pillbox.[1]

In addition to the magnetic term given by Equation (5) due to the generation of the solenoidal electric field, there is also another contribution to the impedance that comes from distortion of the beam-potential electric field by the chamber discontinuity. Because the distorted field is the potential field, rot $\vec{E} = 0$, its longitudinal component can be written as $E_z = -\partial\phi(z)/\partial z$. It makes the following contribution to $\mathcal{E}$:

$$\mathcal{E}_{(e)} = \int_{-\infty}^{\infty} dz E(z) \exp(-ikz)$$

$$= -\int_{-\infty}^{\infty} dz e^{-i\omega z/c} \partial_z \big(\phi(z) - \phi_\infty\big) . \tag{6}$$

In Equation (6) we have taken into account that the perturbed field is localized near the discontinuity, and that $\phi(z) \to \phi_\infty$ when $z \to \pm\infty$. Integrating by parts, one finds

$$\mathcal{E}_{(e)} = -i\frac{\omega}{c} \int_{-\infty}^{\infty} dz e^{-i\omega z/c} \big(\phi(z) - \phi_\infty\big)$$

$$\simeq -i\frac{\omega}{c} \int_{-\infty}^{\infty} dz \big(\phi(z) - \phi_\infty\big) . \tag{7}$$

In the last step we used the fact that the wavelength c/ω is large compared to the pipe radius and, therefore, to the size of the region where the perturbed field is localized.

To perform integration in Equation (7) it is convenient to shift the integration path from the axis closer to the wall. If the distance from the pillbox to the integration path is such that $g, h \ll |\vec{R}| \ll b$, where $\vec{R} = (z, x)$ and $x = r - b$, the main component of the perturbed electrostatic potential is a dipole,

$$\phi(z) = \phi_\infty + \phi_{dip}(z) = \phi_\infty + \frac{1}{2\pi\varepsilon_0} \frac{px}{x^2 + z^2} , \tag{8}$$

where the last term corresponds to the electric dipole in radial direction, distributed along the circumference of the chamber cross section, and p is the dipole moment per unit length of the pipe circumference. From Equation (7) we find immediately (for $x < 0$):

$$\mathcal{E}_{(e)} = i\frac{\omega}{c} \frac{p}{2\varepsilon_0} . \tag{9}$$

It is natural to introduce the electric polarizability per unit length α_e of the discontinuity as $p = \varepsilon_0 \alpha_e E_r$, where $E_r = I_0/(\varepsilon_0 c 2\pi b)$ is the beam electric field at the wall. Then the electrostatic contribution to the impedance is

$$Z_{(e)}(\omega) = -\frac{\mathcal{E}_{(e)}}{I_0} = -i\omega \frac{Z_0 \alpha_e}{4\pi bc} . \tag{10}$$

It turns out (see below) that the induced dipole moment for the pillbox is opposite to the radial beam field, i.e., $\alpha_e < 0$, and the electric contribution to the inductance is negative in this case.

Summing up Equations (5) and(10) we find the low-frequency impedance of a discontinuity as a sum of the magnetic and electric terms that are proportional to the magnetic and electric polarizability respectively. This result is analogous to that for the impedance of a pumping hole at low frequencies,[6] which has been derived in a rigorous but more complicated way using the Bethe theory of diffraction by small holes and an expansion over waveguide modes.

3 RECTANGULAR PILLBOX AND STEP

While the calculation of the magnetic polarizability is straightforward, in order to find the electric polarizability we have to solve an electrostatic problem, namely, to calculate the dipole moment induced on the pillbox by a homogeneous electric field. For small discontinuities ($g, h \ll b$) the dipole moment does not depend on b, and one can solve the problem considering the limit $b \to \infty$. In this limit, the cylindrical geometry reduces to the plane one and we have to find the distribution of the potential created by an infinitely long rectangular groove in a perfectly conducting plane wall that is generated by a uniform electric field perpendicular to the wall. This field is in fact the beam electric field at the wall, E_r.

A standard approach for solving this kind of electrostatic problems is to apply the conformal mapping technique, e.g., Reference 7. For the small pillbox the conformal mapping that relates the coordinates (x, y) with the complex variable $\psi + i\phi$ is given by the following equation (see the Appendix for more detail):

$$z + ix = CE\left(-\arcsin\frac{\psi + i\phi}{CuE_r}, u\right) + ih\,, \tag{11}$$

where $C = g/\big(2E(u)\big)$ and the parameter u is defined by the equation

$$\frac{g}{2h} = \frac{E(u)}{K(\sqrt{1-u^2}) - E(\sqrt{1-u^2})}\,. \tag{12}$$

In the equations above, ϕ is the potential, ψ is the electric flux, and K and E are elliptic integrals of the first and second kind (E denotes the incomplete elliptic integral when it has two arguments and the complete integral with one argument). Inverting the dependence given by Equation (11) and taking the imaginary part, one can find ϕ as a function of x and y. From asymptotic expansion of the elliptic integral, which can be easily performed using the integral representation, cf. the Appendix, we find that at large distances, $\sqrt{x^2+z^2} \gg g, h$, the potential is

$$\phi = -E_r\left[x + \frac{C^2}{2}(1-u^2)\frac{x}{x^2+z^2}\right] + \text{const}\,, \tag{13}$$

and hence the electric polarizability is

$$\alpha_e = -\pi C^2(1-u^2) \equiv -ghf(g/h)\,. \tag{14}$$

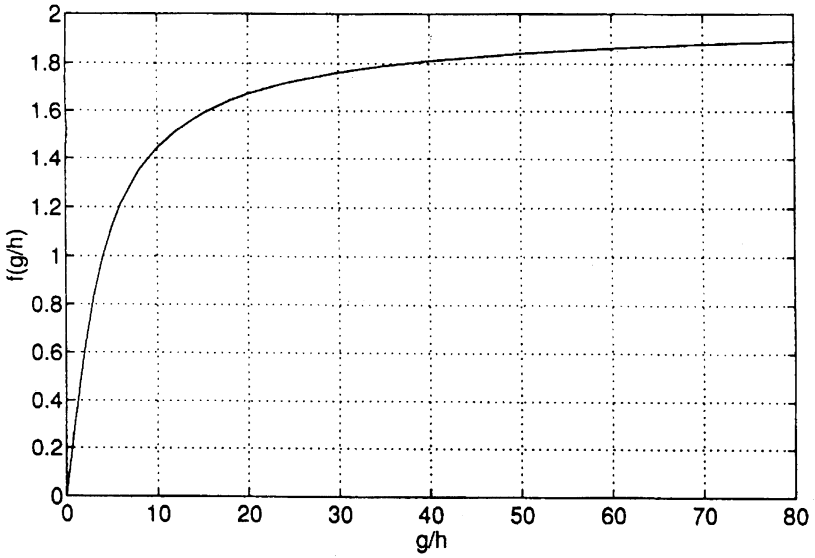

FIGURE 2: The electric polarizability of a pillbox versus the aspect ratio.

The function $f(g/h)$ gives the dependence of α_e on the aspect ratio g/h and is plotted in Figure 2. The function α_e has the following asymptotic behavior:

$$\alpha_e = \begin{cases} -g^2/\pi & \text{when } g \le h \\ -2gh + 2h^2/\pi \,(\ln(2\pi g/h) + 1) & \text{when } g \gg h. \end{cases} \tag{15}$$

The conformal mapping and polarizability for other shapes of the discontinuity (Figures 1(b)–1(e)) are discussed in the Appendix.

Collecting together Equations (5) and (10) and using the asymptotic expansion from Equation (15) we obtain the low-frequency impedance of the small short pillbox ($g \le h$),

$$Z(\omega) = -i\omega \frac{Z_0}{2\pi bc} \left(gh - \frac{g^2}{2\pi} \right), \tag{16}$$

which is inductive. The electric contribution to the inductance is negative and small in this case. The comparison of Equation (16) with numerical computations by means of the ABCI code[8] is shown in Figure 3. As follows from this figure, the electric contribution to the impedance is small but noticeable.

For deeper pillboxes one must correct the above formula, taking into account that the magnetic field in the pillbox varies with radius as $1/r$. When the ratio h/b is not very small, we have to use the exact expression of Equation (3) for the magnetic flux. Performing simple integration, we find that the approximate result $\alpha_m = gh$, which is

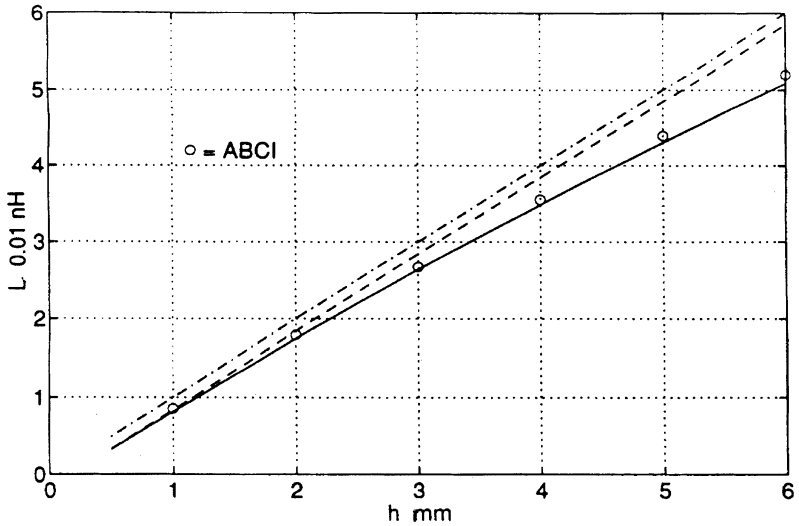

FIGURE 3: The inductance of a deep pillbox versus its depth: without (dash-dotted) and with (dashed) the electric term; with the electric term and smeared magnetic moment (solid). Here pipe radius b=2cm, pillbox length g=1mm.

valid in the limit $h \ll b$, has to be replaced by $\alpha_m = gb\ln(1 + h/b)$ (the solid curve in Figure 3). The impedance Z_m with this logarithm's term coincides exactly with the expression obtained in Reference 1 by the field-matching method. As for the electric term, we do not need such corrections in this case, $g \ll h$, since the electric field is distorted in the region with a typical size of the order of g.

In the opposite extreme, $g \gg h$, the situation is different: the electric and magnetic contributions almost cancel each other, and the low-frequency impedance of the shallow enlargement takes the form

$$Z(\omega) = -i\omega \frac{Z_0 h^2}{2\pi^2 bc} (2\ln(2\pi g/h) + 1) \ , \tag{17}$$

where g should still be below b. The h^2 dependence of the shallow-cavity inductance was found earlier by numerical methods (for example, References 3 and 4), but Equation (17) also gives an additional logarithm-type dependence on the aspect ratio that was hard to extract from fitting in the previous works. Figure 4 shows the comparison of ABCI computations and our results for shallow cavities. Minor differences between the analytical and numerical results for $g \geq b$, especially for the deeper cavity, are explained by the fact that our approach is valid only when $g < b$.

Increasing the length g of the pillbox beyond the value of b, we arrive at the situation corresponding to two separate steps. Apparently, in this limit the impedance will not

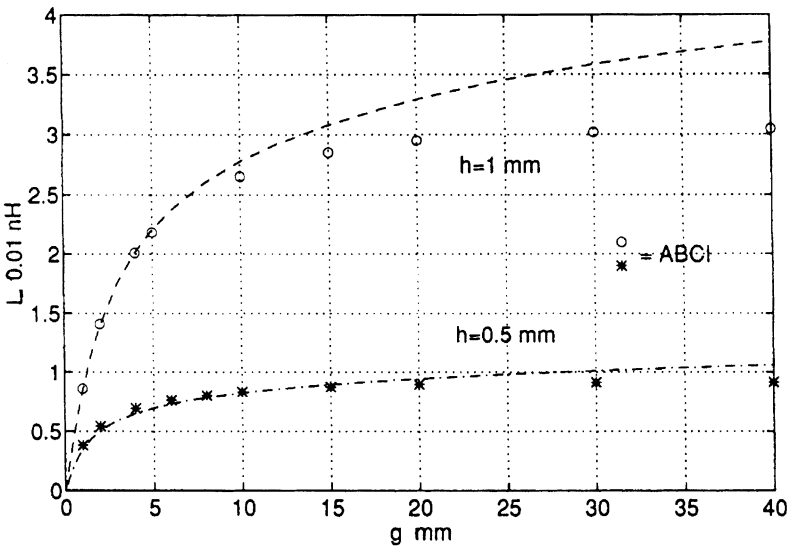

FIGURE 4: The inductance of shallow pillboxes versus the length (b=2cm).

depend on g because a very long pillbox is actually composed of two independent steps — one that increases and one that decreases the beam-pipe radius. It is evident that the transition to the limit of two independent steps occurs when g becomes of the order of pipe radius b, $g \sim b$. Hence, we can estimate the impedance of a step simply by putting $g = b$ in Equation (17) and dividing it by a factor of 2. This gives the following result ($h \ll b$):

$$Z(\omega) = -i\omega \frac{Z_0 h^2}{4\pi^2 bc} \left(2\ln(2\pi b/h) + 1\right) . \tag{18}$$

Since, however, the logarithm already has large ratio $2\pi b/h$ as its argument, the exact value of coefficient c in the substitution $g \mapsto cb$ is not very important; it would make a relatively small correction $\sim \ln c / \ln(2\pi b/h)$ to Equation (18). To check the accuracy of Equation (18), we have compared results given by this formula with numerical results for a single small step obtained by means of the ABCI code. With $b = 2$cm, the analytical and numerical results for $h \leq 1$mm agree within 1%.

It should be noted that, in addition to the imaginary part given by Equation (18), there is also a real part of the step impedance associated with the potential jump through the transition from the broad to the narrow part of pipe. The real part of the impedance is proportional to $\ln(1 + h/b)$ being positive for the transition "narrow-to-broad" and negative in the opposite case. For shallow cavities the contributions to the real part from the two steps exactly cancel each other.

4 OTHER SHAPES OF DISCONTINUITIES

The conformal mappings for a symmetric trapezoid, Figure 1(b), and triangular insertions, Figures 1(d) and1(e), are given in the Appendix. Considering a shallow trapezoid ($h \ll g$) one can find the inductance of a single sloping step (transition) in the same way as that of the abrupt step, Equation (18). The inductance produced by the transition with the slope angle $\theta = \pi\nu$ has the form

$$Z(\omega) = -i\omega\frac{Z_0 h^2}{2\pi^2 bc}\left[\ln\pi\nu\left(\frac{b}{h} - 2\cot\pi\nu\right) + \frac{3}{2} - \gamma - \psi(\nu) - \frac{\pi}{2}\cot\pi\nu - \frac{1}{2\nu}\right], \tag{19}$$

where $\gamma = 0.5772\ldots$ is Euler's constant, $\psi(\nu)$ is the psi-function, and the transition is assumed to be short compared to the chamber radius, i.e. the transition length $l = h\cot\pi\nu \ll b$. The ratio of this inductance to that of the abrupt step ($\nu = 1/2$, Eq. (18)) with the same height is plotted in Figure 5 as a function of the slope angle. It should be noted that Equation (19) transforms into Equation (18) in the limit $\nu \to 1/2$.

In the same way, one can consider discontinuities that protrude inside the chamber, like an iris or a collimator, as in Figure 1(c). It is clear that in this case both the magnetic and electric dipole moments must change sign. It turns out, however, that in this case the electric contribution is larger than the magnetic one, and the low-frequency impedance is again inductive with positive value of the inductance. Making use of conformal mapping in Equation (25) with $\nu = -1/2$, one can find the inductance for an iris of the length g and depth h. When $h \ll g$, the impedance of the iris coincides with that of a shallow cavity, Equation (17). This result seems quite natural and, indeed, was found earlier[3,4] from numerical results. For the case of a thin (or deeper) iris, $g \ll h$, the asymptotic expression for $Z(\omega)$ takes the form

$$Z(\omega) = -i\omega\frac{Z_0}{4bc}\left[h^2 + \frac{gh}{\pi}\left(\ln(8\pi g/h) - 3\right)\right]. \tag{20}$$

Figure 6 shows the comparison of this formula with numerical computations. It is seen that Equation (20), derived in the limit $h \ll b$, works amazingly well even for very deep, narrow irises.

As a bridge between these two analytical asymptotics ($g \gg h$ and $g \ll h$), we give below a formula for the low-frequency impedance of the iris with an arbitrary aspect ratio:

$$Z(\omega) = -i\omega\frac{Z_0}{2\pi c}\frac{gh}{b}F\left(\frac{h}{g}\right). \tag{21}$$

Here function $F(x)$, plotted in Figure 7, is obtained by solving Equations (25)–(32) (see the Appendix) numerically for α_e, with $\nu = -1/2$. Then, adding Equation (10) to the magnetic contribution of Equation (5) with $\alpha_m = -gh$ ($g \ll b$ and $h \ll b$ are assumed, rigorously speaking), we get the formula above. Figure 7 also gives an idea on the accuracy of Equation (21), comparing it with the ABCI results. Pipe radius $b = 2$cm, $h = 1$–15mm, and $g = 2$–8mm were used in the ABCI computations.

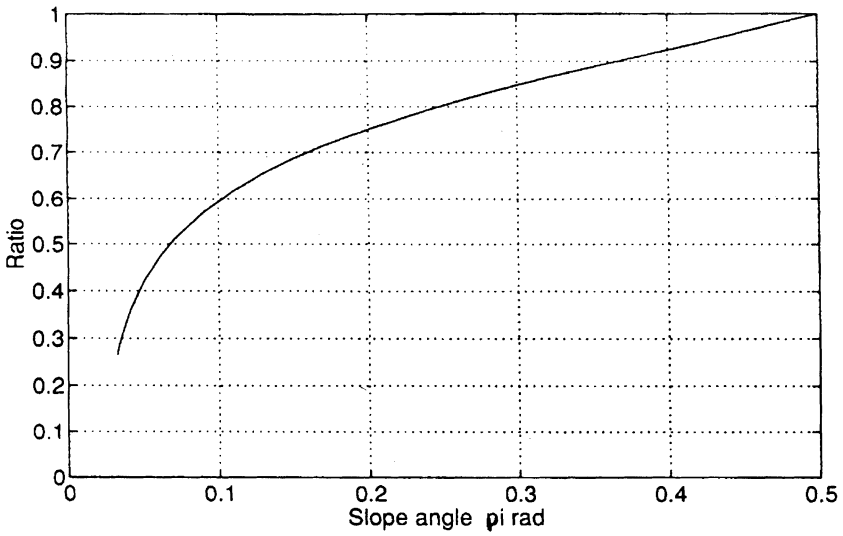

FIGURE 5: The inductance of a shallow sloping step with fixed height versus the slope angle (in units of that for the abrupt step).

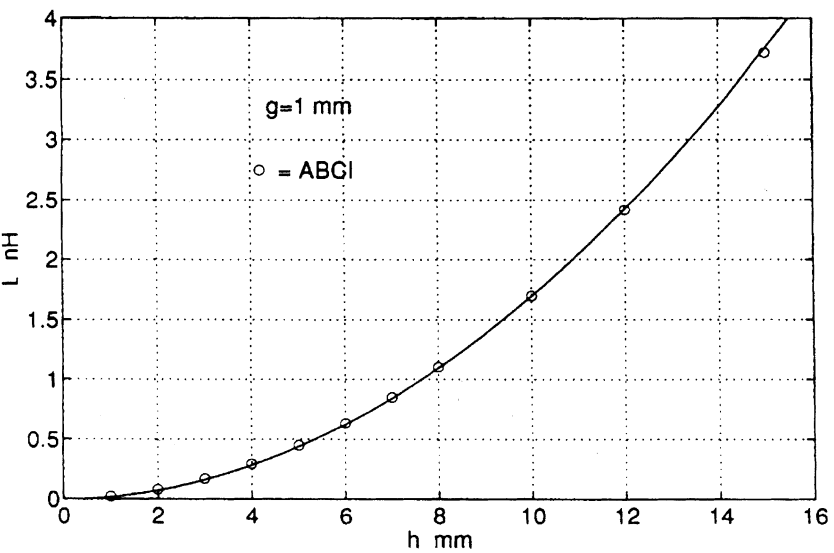

FIGURE 6: The inductance of a narrow iris versus its depth. Pipe radius b=2cm.

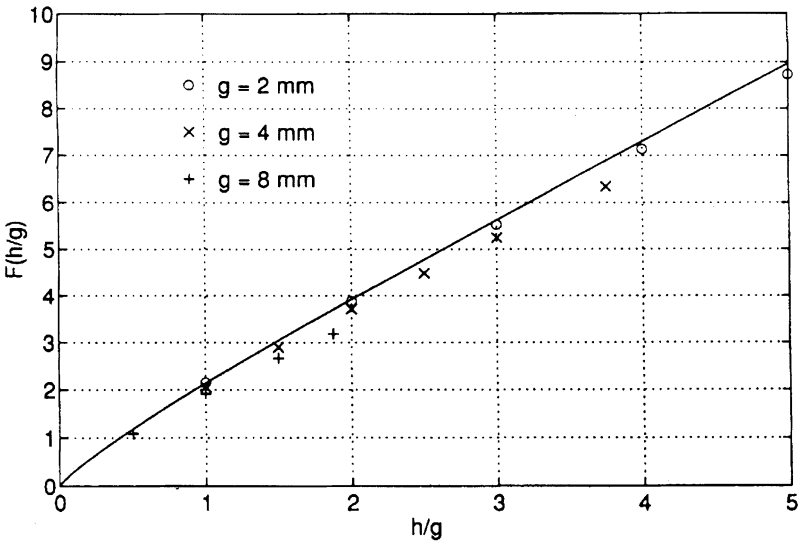

FIGURE 7: The iris inductance dependence on the aspect ratio, see Equation (21).

As another example, we consider discontinuities of a triangle-shaped cross section with height (depth) h and base g, shown in Figures 1(d) and 1(e) (see the Appendix). When $g \ll h$, the low-frequency impedance of such a chamber enlargement is

$$Z(\omega) = -i\omega \frac{Z_0}{4\pi bc}\left(gh - \frac{g^2}{\pi}\right), \tag{22}$$

and that of a triangular iris is

$$Z(\omega) = -i\omega \frac{Z_0}{4bc}\left[h^2 + \frac{2gh}{\pi}(1 - \ln 2)\right]. \tag{23}$$

For the case of shallow triangular perturbations, $h \ll g < b$, both the enlargement and contraction of the chamber have the same inductance,

$$Z(\omega) = -i\omega \frac{Z_0 h^2 2 \ln 2}{\pi^2 bc}, \tag{24}$$

which is independent of g.

5 LARGE CAVITIES

Thus far, we have assumed that the dimensions of the discontinuities on the beam pipe were much smaller than the beam-pipe radius. We can relax this restriction and apply our method for large axisymmetric discontinuities. However, as before, the wavelength will be assumed

to be large compared to a typical discontinuity size, which now can be of the order of, or larger than, the pipe radius.

The magnetic contribution for a large pillbox can be easily found for an arbitrary shape of the boundaries if we use the exact expression of Equation (3) of the magnetic flux while calculating the magnetic polarizability.

As for the electric contribution, we have to solve the electrostatic problem exactly without invoking the plane approximation. This part of the problem has been solved using a standard electrostatic code, POISSON.[9] After having calculated the potential distribution produced in an axisymmetric structure by a linear charge located on the chamber axis, we integrate it numerically at $r = b$ according to Equation (7). Effectively, this integration involves only a part of the integration path that crosses the cavity opening, since on the wall $\phi(z) = \phi_\infty$. For the illustration of the method, we have calculated the inductance of the cavity having the shape shown in Figure 1(a) with the length $g = 5$cm and depth $h = 3$cm on the pipe of radius $b = 2$cm. The magnetic part of the impedance is $L_{(m)} = Z_0 g \ln(1+h/b)/(2\pi bc) = 9.2$nH. The electric one (from POISSON computations) is $L_{(e)} = -3.5$nH, which amounts to the total impedance $L = 5.7$nH. The ABCI code gives us a very close value, $L = 5.78$nH.

As one more example, we have considered a cavity of the same shape and size as above, but shielded from the beam pipe by a screen in such a way that only an axisymmetric short gap of length 0.4cm couples the cavity and beam pipe. In such a layout the induced electric dipole is very small and the inductance has to be due only to the magnetic term, $L \simeq L_{(m)} = 9.2$nH, while the ABCI result is $L = 9.4$nH. These two examples show that our approach works well for large discontinuities also.

6 CONCLUSIONS

We have developed a method that allows the calculation of the low-frequency impedance for a small discontinuity of the beam vacuum chamber. There are two contributions to the impedance — the electric and the magnetic, which have opposite signs — but the resulting low-frequency impedance is always inductive. This approach gives a clear physical picture and allows us to reproduce and explain results obtained earlier from numerical simulations. In many cases, simple analytical formulae for the low-frequency impedance are derived.

We have to emphasize here that being perturbative in small parameters g/b and h/b, our method includes all the important terms in the lowest order so that neglected terms are much smaller than those retained. In that sense, our result is accurate in the range of its validity.

We have also demonstrated that our method allows us to compute easily the low-frequency impedance for large cavities. As a future generalization we intend to apply the approach to study the impedance of small discontinuities at frequencies above the cut-off frequency. We believe that in this frequency range the idea of effective dipole moments will be fruitful as well.

REFERENCES

1. E. Keil and B. Zotter, *Particle Accelerators*, **3**, 11–20 (1972).
2. T. Weiland, NIM, **212**, 13–21 (1983).

3. K. Bane, *European Particle Accelelerators Conference.* (Rome, 1988). World Scientific, Singapore, **2**, 637–9 (1989).
4. S.S. Kurennoy and S.V. Purtov, *Particle Accelerators*, **36**, 223–240 (1992).
5. S. Heifets and S. Kheifets, *Rev. Mod. Phys.*, **63**, 631–674 (1991). S.S. Kurennoy, Report CERN SL/91-31 (AP), Geneva, 1991; *Phys. Part. Nucl.*, **24**, 380 (1993).
6. S.S. Kurennoy, *Particle Accelerators*, **39**, 1–13 (1992).
7. P.M. Morse and H. Feshbach, *Methods of Theoretical Physics*, McGraw-Hill, NY (1953) p.1215.
8. Y.H. Chin, Report CERN SL/92-49 (AP), Geneva (1992).
9. K. Halbach, in *Proceedinds of the Second International Conference on Magnet Technology*, Oxford, UK (1967) p.47.
10. M. Abramowitz and I.A. Stegun (eds.) *Handbook of Mathematical Functions*, Dover Publ., NY, 1965.

APPENDIX : CONFORMAL MAPPING

The conformal mapping from the upper half-plane $w = \psi + i\phi$ on the plane $v = z + ix$ for the discontinuity having the symmetric trapezoidal shape with height h, base g, and slope angle $\pi\nu$, where $g \geq 2h \cot \pi\nu$ (see Figure 1(b)), can be derived using the standard technique of the Schwarz-Cristoffel transformation. Choosing the point correspondence between w- and v-planes as $(0, 1) \leftrightarrow (0, g/2)$, $(0, u) \leftrightarrow (g/2 - h \cot \pi\nu, h)$, where $0 \leq u \leq 1$, and taking into account the problem symmetry yields the following conformal mapping:

$$v = C \int_0^w d\xi \left(\frac{\xi^2 - 1}{\xi^2 - u^2} \right)^\nu + ih \,, \tag{25}$$

where transformation parameters C and u satisfy the simultaneous equations:

$$\frac{g}{2} - h \cot \pi\nu = C \int_0^u d\xi \left(\frac{1 - \xi^2}{u^2 - \xi^2} \right)^\nu \,; \tag{26}$$

$$h = C \sin \pi\nu \int_u^1 d\xi \left(\frac{1 - \xi^2}{\xi^2 - u^2} \right)^\nu \,. \tag{27}$$

The integrals in the equations above can be expressed in terms of the Gauss hypergeometric function ${}_2F_1$ and gamma-function Γ (see definitions in Reference 10). Solving these equations with respect to C gives

$$C = \frac{2hu}{\pi\nu(1 - u^2) {}_2F_1(\frac{1}{2}, 1 - \nu, 2, 1 - u^{-2})} \,, \tag{28}$$

where u is defined as a root ($0 \leq u \leq 1$) of the equation

$$\frac{g}{2h} \sin \pi\nu - \cos \pi\nu = \frac{\sqrt{\pi}}{\Gamma(\frac{3}{2} - \nu)\,\Gamma(1 + \nu)} \frac{u^{2-2\nu}}{1 - u^2} \frac{{}_2F_1(\frac{1}{2}, -\nu, \frac{3}{2} - \nu, u^2)}{{}_2F_1(\frac{1}{2}, 1 - \nu, 2, 1 - u^{-2})} \,. \tag{29}$$

Asymptotics at $w \to \infty$ of the integral in the RHS of Equation (25) can be obtained easily:

$$v = Cw + const + C \frac{\nu(1 - u^2)}{w} + \ldots \tag{30}$$

Reversing this relation with account of $w \to \infty$ and $v \to \infty$ yields

$$w = \frac{v}{C} + const_1 - C \frac{\nu(1 - u^2)}{v} + \ldots \tag{31}$$

The first term here corresponds to an unperturbed electric field, and the last one gives the dipole contribution. From this asymptotic behavior we can obtain the electric polarizability per unit length of circumference (see discussion in Sections 2 and 3).

$$\alpha_e = -2\pi\nu C^2(1-u^2)\,. \tag{32}$$

In the case of a pillbox, Figure 1(a), $\nu = 1/2$, and hypergeometric functions ${}_2F_1$ in Equation (29) are reduced to complete elliptic integrals.[10] As a result, Equation (29) transforms into Equation (12) of Section 2. Respectively, Equation (25) for $\nu = 1/2$ yields Equation (11) with the integral representation of incomplete elliptic integral $E(\arcsin(w/u), u)$, up to the potential normalization (we use the dimensionless variables in the Appendix, unlike the main text).

It is worth noting, that Equations (25) and (29) can be applied not only for chamber enlargements but also for chamber contractions if we replace $h \to -h$ ($h > 0$) for $\nu < 0$. In this case, $\nu = -1/2$ corresponds to an iris, Figure 1(c).

The particular case $u = 0$ ($g = 2h\cot\pi\nu$) gives conformal mapping for triangular perturbations, Figures 1(d) and 1(e). In this case, conformal mapping of Equation (25) takes the form

$$v = \frac{(g/2 - ih)\Gamma(1/2)}{2\Gamma(3/2-\nu)\,\Gamma(1+\nu)} w^{1-2\nu}\,{}_2F_1\left(\frac{1}{2}-\nu, -\nu, \frac{3}{2}, w^2\right) + ih\,.$$

Hypergeometric functions in Equation (29) transform now into combinations of gamma-functions, and the electric polarizability of Equation (32) is reduced to

$$\alpha_e = -2\nu\left[\frac{\pi h}{\sin\pi\nu\Gamma(1/2-\nu)\,\Gamma(1+\nu)}\right]^2\,. \tag{33}$$

To derive the impedance of a shallow and short transition (see Section 4), we consider the limit $g \gg h$ of Equation (29), with ν fixed, $0 < \nu \leq 1/2$ (more rigorously, one should keep $\pi\nu \gg 2h/g$, and this case is not reduced to shallow triangular perturbations). In this limit, $u \to 1$ and we can use in Equation (29) the linear transformations for hypergeometric functions[10] to obtain the expansions over small parameter $\delta \equiv 1 - u^2$, $0 < \delta \ll 1$, as follows:

$$\begin{aligned}
{}_2F_1\left(\frac{1}{2}, 1-\nu, 2, 1-u^{-2}\right) &= 1 - \frac{1-\nu}{4}(\delta+\delta^2) + \frac{(1-\nu)(2-\nu)}{16}\delta^2 + \ldots \\
{}_2F_1\left(\frac{1}{2}, -\nu, \frac{3}{2}-\nu, u^2\right) &= \frac{\Gamma(3/2-\nu)}{\Gamma(3/2)\,\Gamma(1-\nu)} \times \\
&\quad \times\left[1 - \frac{\nu}{2}\delta\,(\ln\delta + \gamma + 1 - 2\ln 2 - \psi(1-\nu) + \ldots)\right],
\end{aligned} \tag{34}$$

where $\gamma = 0.5772\ldots$ is Euler's constant, $\psi(x)$ is the psi-function.[10] Substituting these expansions into Equation (29) and solving it with respect to δ, we get, after some algebra, from Equation (32) the electric polarizability

$$\alpha_e = -2(gh - h^2 \cot \pi\nu) + \frac{4h^2}{\pi}\left[\ln \pi\nu \left(\frac{g}{h} - 2\cot \pi\nu\right) + \frac{3}{2} - \gamma - \psi(\nu) - \frac{\pi}{2}\cot \pi\nu - \frac{1}{2\nu}\right]. \tag{35}$$

Putting it into Equation (10) and adding the magnetic contribution, Equation (5), which just cancels the first term, proportional to the trapezoid area, in the expression above, leads to Equation (19) for the impedance of a shallow transition.